Regimes of Exciton Transport in Molecular Crystals in the Presence of Dynamic Disorder

Juan Aragó, Alessandro Troisi*

Department of Chemistry and Centre for Scientific Computing, University of Warwick, Coventry CV4 7AL, UK

Thermal motions in molecular crystals cause substantial fluctuation of the excitonic coupling between neighboring molecules (dynamic disorder). We explore the effect of such fluctuation on the exciton dynamics in two limiting cases, exemplified by the crystals of anthracene and a heteropentacene derivative. When the excitonic coupling is small in comparison with the electron phonon coupling, the exciton diffusion is incoherent and the inclusion of excitonic coupling fluctuation does not alter the exciton physics but can improve the agreement between computed and experimental diffusion coefficients. For large excitonic couplings, when the transport becomes coherent, the thermal motions determine the diffusivity of the exciton, which can be several orders of magnitude larger than in the incoherent case. The coherent regime is less frequent but potentially of great technological importance.

1. Introduction

Exciton diffusion in molecular materials is a fundamental physical process taking place in many organic electronic devices including light emitting diodes and solar cells. For example, a long exciton diffusion length is a prerequisite for efficient organic solar cells, where excitons should diffuse to a donor-acceptor interface to initiate the process of charge separation and, consequently, the generation of photocurrent.

In general, regardless of the exciton diffusion mechanism, the diffusion of molecular excitons is mainly driven by the excitonic coupling (J) between the excited states localized on the molecular units (Frenkel excited states).[1,2] The excitonic coupling can be separated into short-range (exchange and overlap) and long-range (Coulombic) contributions.[3–6] The latter is often the only term considered to investigate exciton transport in molecular aggregates (the only term, for instance, in the popular Förster theory[7] for excitation energy transfer), an approximation justified when the interacting molecular moieties are separated by long intermolecular distances.[8] However, short-range contributions become relevant in organic molecular crystals whose intermolecular closer contacts are in the 3.5–4.5 Å range.[9] Additionally, molecular crystals possess a large number of low frequency intermolecular vibrations that cause a relatively large displacement of one molecule respect to their neighbors (dynamic disorder).[10] In contrast to long-range excitonic contributions, short-range excitonic interactions (exchange and overlap effects) are extremely sensitive to the mutual orientation of the molecule and, therefore, can undergo significant fluctuations owing to the thermal molecular motions. It has been recently shown that the thermal motion of the molecules around their equilibrium position gives rise to large fluctuations of the excitonic coupling J, sometimes referred to as non-local exciton-phonon coupling.[11]

The fluctuation of excitonic couplings in molecular solids is a relatively intuitive effect, especially when compared to the analogous fluctuation of the hopping integral in charge transport,[12,13] but it has not received much attention in the literature despite its great importance for the quantitative description of exciton transport. Renaud and Grozema have recently shown that intermolecular vibrations can speed up singlet exciton fission in perylenediimide crystals due to the modulation of the couplings.[14] Stangl *et al.* have experimentally detected a large temporal fluctuation of the excimer-like interactions between π-conjugated chromophores at the molecular level; i.e., they observed a scatter of the photoluminescence lifetimes of almost a third of the mean lifetime value for the π-conjugated dimers with the short intermolecular contacts, which was associated to the molecular dynamics of the chromophores. The authors therefore suggested that the dynamic heterogeneity in strong interchromophore couplings must be accounted for to gain insights into the flow of excitation energy in bulk optoelectronic systems.[15]

The description of the exciton transport in organic molecular crystals is particularly simple in two limiting transport regimes (coherent and incoherent).[2] In the coherent regime, the excitonic coupling is much larger than the local exciton-phonon coupling (reorganization energy) and the exciton wavefunction is delocalized over the aggregate.[1] In the opposite (incoherent) regime, the exciton coupling between adjacent molecules is much weaker than exciton-phonon coupling, and the exciton wavefunction, localized on a molecular unit, diffuses via a series of exciton hopping events between neighboring molecules. In both limits it is often assumed that J is a constant,[16–18] i.e. not dependent on time or, equivalently, on the nuclear displacement (Condon approximation). Nevertheless, it is now clear[14,15] that the thermal fluctuation of the excitonic couplings in molecular crystals or aggregates is an effect that should become

part of any quantitative exciton transport theory. The formulation of such a theory depends on the characteristic timescale of the excitonic coupling fluctuations and their strength. The limit of J fluctuations that are faster than any other timescale can be studied in the classical Haken–Strobl–Reineker model,[19,20] whereas the limit of J fluctuations slower than any other timescale is a particular case of exciton transport in a statically disordered system.[21] For weak fluctuations, i.e. if their amplitude is much smaller than their average value, one can adopt exciton-polaron band renormalization theories.[22] According to the computational study of ref. [11] none of these limits is appropriate for exciton transport in the most studied materials, since the fluctuations have a large amplitude at room temperature and a characteristic timescale comparable to that of the exciton diffusion.

In this paper, we explore the effect of the excitonic coupling fluctuation due to the thermal nuclear motions on the exciton dynamics in molecular crystals without assuming that the fluctuation is weak or that its timescale is different from that of the exciton diffusion. However, this effect is rather different in molecular systems if the local exciton-phonon coupling is strong (leading to localized excitons) or weak (leading to delocalized excitons). The regime intermediate between strong and weak exciton-phonon coupling is by itself an interesting and complicated problem. Nevertheless, as here we are concerned with the effect of the fluctuation on the exciton transport, we consider two more extreme examples which are definitely in the localized or delocalized regime.

Anthracene crystal (Figure 1) is our model for exciton transport in the localized exciton regime. It has been selected because it is a good model for a wide range of active donor materials in the context of organic electronics and its exciton transport properties have been experimentally[23–26] and theoretically[27–31] characterized. The

relatively strong exciton-phonon coupling, due to its small size, is already evident from the absorption spectrum. Moreover, anthracene is the best model system within the family of oligoacenes to study the role of the excitonic coupling fluctuation in the exciton transport for further reasons. First, the nature of the lowest-energy excitations in anthracene (Frenkel excitons, FE) is simpler than in the case of longer oligoacenes (tetracene and pentacene), where the lowest-energy excitons are described by a significant mixture of FE and charge-transfer (CT) excited states.[32] Second, tetracene and pentacene (especially the latter) present multiexcitonic states in the vicinity of the FE excited states and, thus, can undergo ultrafast singlet exciton fission.[33,34] One can therefore explore the effect of exciton coupling fluctuation in anthracene, without the complications generated by the presence of other excited states.

As a model for exciton transport in the delocalized regime we consider DCVSN5 (dicyanovinyl-capped *S*,*N*-heteropentacene, Figure 2), a novel molecule which is a promising donor candidate for small molecule organic solar cells (SM-OSCs).[35] This donor material in conjunction with a fullerene (acceptor) have been implemented in a photovoltaic cell with efficiencies as high as 6.5%, which is a remarkable efficiency for SM-OSCs.[36] Compounds with a similar acceptor-donor-acceptor (A-D-A) backbone have shown great promise as electron donor materials for high efficiency in single-junction and tandem SM-OSCs.[37–41]

2. Computational Methods

To evaluate the time fluctuation of the excitonic coupling owing to the thermal motions in anthracene and DCVSN5 crystals, we have adopted a combined molecular dynamics (MD) and quantum chemical (QC) approach similar to that used in ref [11]. We have built a 3 × 3 × 3 supercell of the anthracene crystal by replicating the unit cell along the

crystallographic axes *a*, *b*, and *c*, respectively. A 2 × 2 × 2 supercell was built for DCVSN5. The MD simulation at constant temperature (300 K) was run using the MM3 force field[42] for the case of anthracene. In the case of DCVSN5, we developed a force field that reproduces the equilibrium structure and the forces around the equilibrium position computed at the B3LYP/6-31G** level.[43] The electrostatic intermolecular interaction was modelled by point charges (evaluated via the CHELPG procedure[44]) whereas the non-bonded interactions were described by CHARMM parameters[45,46] (see the Supporting Information for further details about the force field for DCVSN5). The integration time was set to 1 fs and 2050 snapshots every 50 fs were taken. The Tinker program package[47] was used to carry out the MD calculations.

To evaluate the time evolution of the excitonic coupling in anthracene and DCVSN5, two clusters consisting of six and seven anthracene and DCVSN5 molecules, respectively, were extracted from each MD snapshot and the excitonic couplings for three different A- and B-type anthracene dimers (Figure 1) and two different A-, B- and C-type DCVSN5 dimers (Figure 2) were computed. The excitonic couplings were computed by means of a two-level diabatization scheme described in ref [48], which employs atomic transition charges (ATCs) as the molecular property for the diabatization process. Within this diabatization procedure, both long and short range excitonic coupling elements are computed on equal footing. It is necessary to clarify that we are not using ATCs to evaluate only the Coulombic term of the excitonic coupling[32,49,50] but the total excitonic coupling (diabatization scheme). No environment polarization effects has been included having verified, for the case of neighboring dimers in tetracene, that the excitonic coupling between FE excited states changes very little when the relative dielectric constant is changed in the 1-7 range.[48] Polarization

effects become important for the excitonic coupling between molecules at longer distance and when CT states are involved.

The excitation energies and the atomic transition charges for the dimers and monomers of anthracene and DCVSN5 were calculated in the framework of the time-dependent density functional theory by using the long-range corrected ωB97X-D[51,52] density functional and the 3-21G* basis set.[53] Note that the differences with the excitonic couplings computed with the larger 6-31G* basis set were on average less than 10%.[11] ωB97X-D was selected because it has proven to provide an accurate description of valence and charge-transfer excitations in molecular dimers and avoids the typical underestimation of the charge-transfer excitations found in standard hybrid density functionals.[54] Reorganization energies and the Huang-Rhys factors were also computed at ωB97X-D but with the larger 6-31G** basis set (see Supporting Information). All TDDFT calculations have been performed by using the Gaussian 09 program package.[55]

3. Results and Discussion

3.1 Fluctuation of the Excitonic Couplings

Figure 1 shows the typical herringbone crystal packing of anthracene (space group $P2_1/a$, with two translationally inequivalent molecules per unit cell). The strongest excitonic interactions take place between adjacent molecules in the *ab* plane.[28,30] In this plane, two different molecular dimers with the closest intermolecular contacts can be identified; the slipped π-stacked (A) and the tilted (B) dimers (Figure 1b).

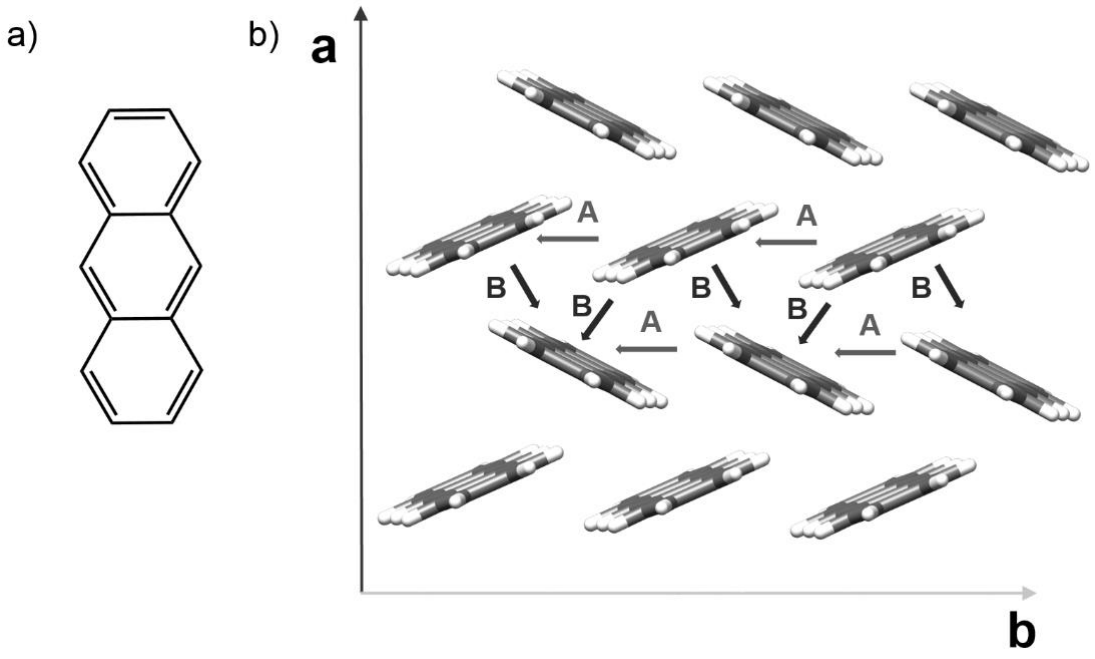

Figure 1. Chemical structure (a) and herringbone crystal structure (b) in the *ab* plane of anthracene. The most relevant dimers for the exciton transport in the crystal *ab* plane are labeled.

DCVSN5 arranges in antiparallel π-stacked columns where short intermolecular distances around 3.5 Å can be found within a column (Figure 2c). Intercolumnar interactions are also seen (Figure 2b and 2d), where DCVSN5 can interact with four neighboring molecules via interactions between the cyano groups of one molecule and the vinylic/heteroaromatic hydrogens or sulphur atoms of the other one. Only the neighboring molecular pairs with the closest intermolecular contacts are selected to evaluate the excitonic couplings (dimers A, B, and C). Dimer A corresponds to the antiparallel π-stacked pair (Figure 2c) within a π-stacked column whereas dimers B and C are molecular pairs between columns (Figure 2d).

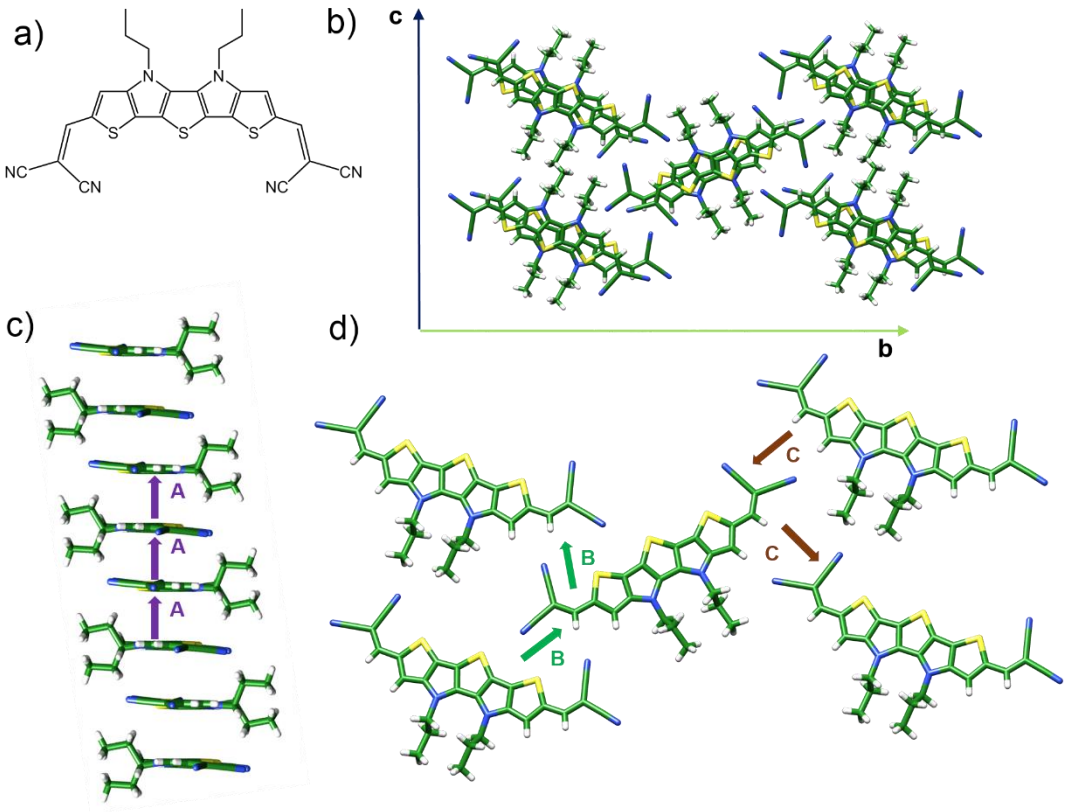

Figure 2. Chemical structure (a) and crystal packing in the *cb* plane of DCVSN5. The most relevant dimers for the exciton transport within an antiparallel π-stacked column (c) and between columns (d) are labeled.

The time evolution and the distribution of the excitonic couplings computed for the two anthracene dimers (A and B) and the three DCVSN5 dimers (A, B and C) are shown in Figure 3. The excitonic couplings are approximately normally distributed in both materials. The average excitonic coupling $\left(\langle J \rangle\right)$ and the standard deviation $\left(\sigma_J\right)$ at 300 K resulting from the combined MD and QC approximation are -0.035 ± 0.008 and -0.005 ± 0.017 eV for the slipped π-stacked and tilted dimer of anthracene, respectively. The excitonic couplings for anthracene dimers, computed here by means of atomic transitions charges, are very similar to those previously reported and evaluated via transition dipole moments.[11] For DCVSN5 (Figure 3, right), the largest

excitonic coupling is obtained for the antiparallel π-stacked molecular pair with $\langle J \rangle$ and σ_J values of –0.200 and 0.027 eV, respectively. Dimers B and C exhibit similar distributions of the excitonic couplings with $\langle J \rangle$ and σ_J values of 0.018 ± 0.008 and 0.032 ± 0.005 eV, respectively. It should be noted that the modulation of the excitonic coupling introduced by the thermal motions of nuclei in both anthracene and DCVSN5 is in general of the same order of magnitude as the average excitonic couplings. To identify the characteristic timescale of the excitonic coupling fluctuation, the Fourier transformation of the autocorrelation function $\langle \delta J(0) \delta J(t) \rangle$ has been computed and is also shown in Figure 3 for anthracene and DCVSN5 dimers (the deviation from the average excitonic coupling has been defined as $\delta J(t) = J(t) - \langle J(t) \rangle$). Figure 3 reveals that low-frequency vibrations below 100 cm^{-1}, and therefore essentially classical in nature, are responsible for the large modulation of the excitonic coupling for both anthracene and DCVSN5 molecular pairs. For dimers B and C of DCVSN5 some intense features appear above 200 cm^{-1}. However, these dimers will play a less relevant role for the overall exciton transport due to their much smaller excitonic couplings.

It is worth pointing out that the largest excitonic coupling in DCVSN5 is about one order of magnitude larger than the value commonly computed for organic crystals. The main cause is the large transition dipole moment (14.1 Debye) directly related to the Coulombic term of the excitonic coupling (to be compared with the value of 2.4 Debye for anthracene, typical of the oligoacene series).

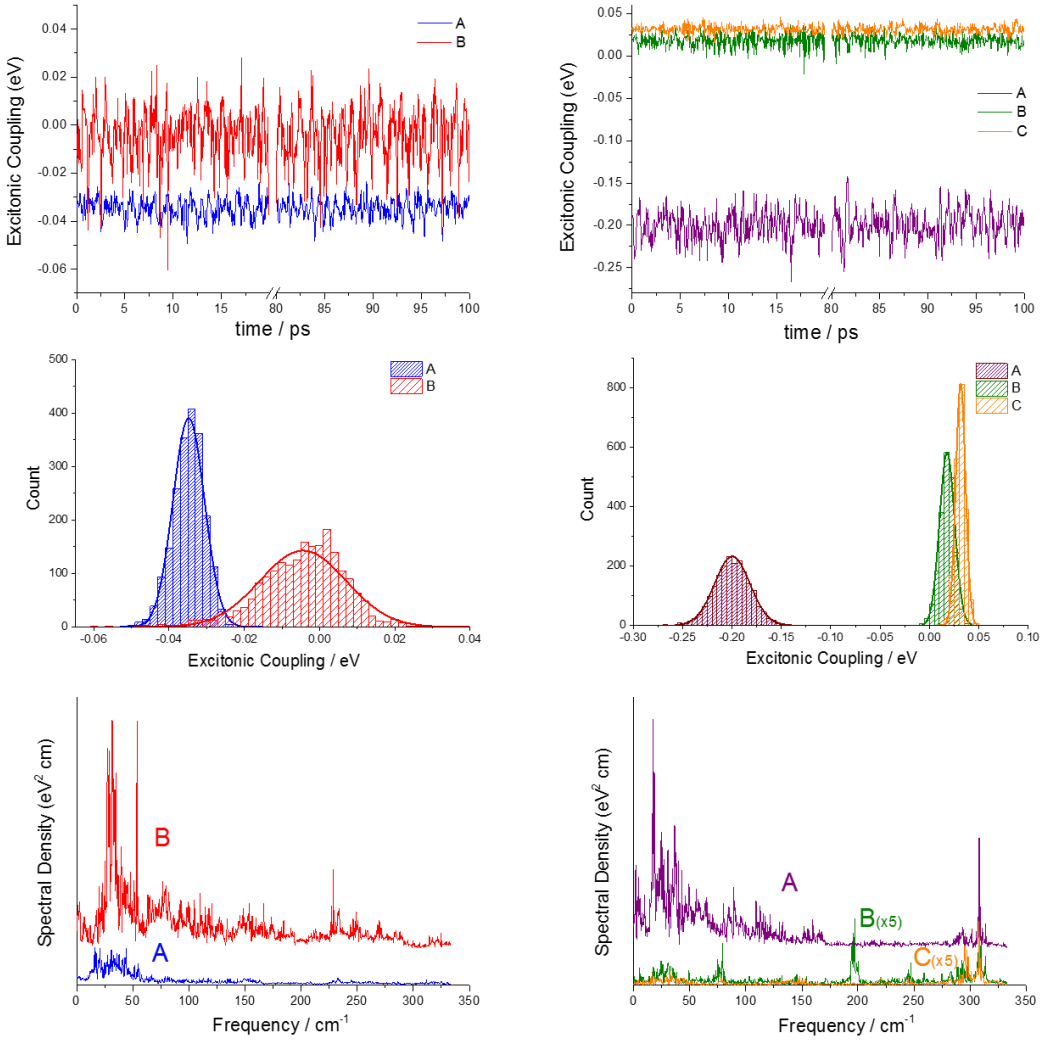

Figure 3. Time evolution (top) and distribution (middle) of the excitonic couplings as well as the Fourier transformation of the autocorrelation function of the excitonic couplings (bottom) computed at 300 K for the anthracene dimers A and B (left), and DCVSN5 dimers A, B and C (right). The intensity of the Fourier transformation graphs for DCVSN5 dimers B and C was multiplied by five for clarity.

The electronic structure origin of the excitonic coupling fluctuation was previously analyzed for the case of anthracene.[11] We had verified that, by removing the short-term contribution, the fluctuations are of much smaller amplitude suggesting that they originate both from the fluctuation of the Coulombic term and the fluctuation of the

short range contribution. Our computational results clearly reveal that the magnitude of the fluctuation (similar to the average value) and the timescale of the vibrations responsible for the fluctuation (around 1 ps close to the timescale for exciton diffusion) prevent the use of the classical Haken–Strobl–Reineker model[19,20] (J fluctuations are not faster than any other timescale) or the exciton-polaron band renormalization theory[22] (the fluctuation is not much smaller than their average value). In this context, we will employ theoretical models for the exciton transport (Section 3.3 and 3.4) capable of accounting for the fluctuation of the excitonic couplings in the appropriate regime.

3.2 Local Exciton-Phonon Coupling

In an exciton transfer process, the reorganization energy[56] (λ) consists of two contributions that reflect the molecular relaxation energies of one molecule (which is excited) going from the fully relaxed ground state to the electronic excited state and a neighboring molecule (which is de-excited) evolving in the opposite manner (see Supporting Information). More generally, the coupling between the electronic states and the phonons in molecular crystals is known as the local exciton-phonon coupling.

The impact of excitonic coupling modulation on the exciton transport depends on the strength of the local electron-phonon coupling, quantified by the reorganization energy. In the case where λ is much larger in comparison with the (average) excitonic coupling, the exciton is highly localized (on one molecule) and the exciton transport takes place by (incoherent) hopping regardless of the amplitude of the excitonic coupling fluctuation. In contrast, for λ smaller or comparable to the excitonic coupling, excitons can be delocalized over many molecules and the transport mechanism depends on the

amplitude of the excitonic coupling fluctuation. Evaluating λ is therefore a prerequisite to identify the plausible regimes of exciton transport in a given molecular crystals.

The reorganization energy of anthracene is calculated to be 0.589 eV at ωB97X-D/6-31G** whereas $\left|\langle J \rangle\right|$ is found to be in the 0.005–0.035 eV range (Figure 3). Therefore, the exciton transport in anthracene crystals is expected to take place in the incoherent regime, in agreement with several theoretical and experimental studies.[30,31,57,58] For DCVSN5 we estimate instead λ to be 0.328 eV, a figure comparable with the excitonic coupling along the antiparallel π-stacked pair (–0.200 eV) and for which one cannot assume incoherent hopping as the transport mechanism (see below).[31]

3.3 Exciton transport in the incoherent regime: the case of anthracene

The strong reorganization energy in anthracene supports the formation of excitons localized on a single molecule with a barrier of $\sim\lambda/4$ = 0.147 eV for the exciton hopping between neighboring molecules. Since the excitonic coupling between initial and final states is much smaller than this barrier (whether the coupling fluctuation is taken into account or not), the hopping transition can be studied as a non-adiabatic reaction using time dependent perturbation theory. In the most common theories the validity of the Condon approximation is assumed, i.e. the coupling between initial and final states is constant (in time or nuclear coordinates). In this case, however, we need to resort to a formulation of non-adiabatic transition rate that takes into account the role of fluctuation of electronic coupling (non-Condon effects).[59–63] The expression of the rate is simpler when the non-Condon effects are due to classical modes, i.e. modes whose energy is lower than the thermal energy. We have shown above for the case of anthracene (Section 3.1) that only low-frequency vibrations in the 20–75 cm^{-1} range are responsible for the modulation of excitonic couplings. Under these conditions the exciton hopping

rate between two molecules, whose averaged squared excitonic coupling is $\langle J^2 \rangle$, can be expressed as:[64]

$$k = \frac{2\pi}{\hbar}\langle J^2 \rangle \sqrt{\frac{1}{4\pi\lambda_c k_B T}} \sum_w P(w) \sum_{w'} \left| FCI_{ww'}(S^{eff}) \right|^2 \exp\left[-\frac{(\lambda_c + (w'-w)\hbar\omega^{eff})^2}{4\lambda_c k_B T} \right] \quad (1)$$

$\langle J^2 \rangle$ incorporates the effect of the thermal fluctuation since $\langle J^2 \rangle = \langle J \rangle^2 + \sigma_J^2$. λ_c, k_B and T correspond to the classical reorganization energy, the Boltzmann constant and temperature, respectively. $P(w)$ is the probability that a vibronic state w on a particular FE excited state is occupied at a certain temperature. $FCI_{ww'}(S^{eff})$ denotes the Franck-Condon integral between the vibrational states w and w' on the FE excited state of molecule 1 and 2, respectively. The Franck-Condon integral depends on the Huang-Rhys factor S^{eff}, which describes the relative displacement along an effective quantum normal mode with energy $\hbar\omega^{eff}$ and is related to the quantum component of the reorganization energy as $\lambda_q = S^{eff}\hbar\omega^{eff}$. The total reorganization energy for the exciton transfer is therefore the sum of a classical and quantum contribution ($\lambda = \lambda_c + \lambda_q$). The above rate expression (eq 1) is very similar to that known as the Marcus-Levich-Jortner rate[65] for electron-transfer processes.

Eq. 1 neglects the instantaneous differences between rates due to different electronic coupling and contains a squared average coupling. This is only valid when the timescale of the coupling fluctuation is not much slower than the exciton transfer time,[63] a condition satisfied for the case of anthracene (where they are both of the order of 1 ps). In practice, in the time between two hops the coupling explores a large range of values. In the opposite limit of slow fluctuations one should consider a distribution of hopping rates between distinct pairs of molecules, as done for example in ref. 21.

All the parameters that enter in the exciton-transfer rate can be computed. Excitonic couplings for anthracene were presented in Section 3.1. The total exciton reorganization energy for an exciton transfer between two anthracene molecules was given in Section 3.2 (0.589 eV).[31] The quantum component of the exciton reorganization energy can be estimated from the Huang-Rhys *S* analysis computed for the bright $S_0 \rightarrow S_1$ electronic transition of an isolated anthracene molecule (Figure S1). Figure S1 clearly shows two high-frequency vibrations at 1482 and 1650 cm^{-1} with the largest *S* values. These normal modes correspond to the typical stretching vibrations of the C-C/C=C bonds of the π-conjugated backbone[66] and cannot be treated classically at room temperature. Nevertheless, the quantum reorganization energy of these high-frequency vibrations can be in overall captured by selecting an effective normal mode, which is set to coincide with the normal mode with the largest *S* ($\hbar\omega^{eff} = 1482$ cm^{-1} with $\lambda_{S_0 \rightarrow S_1} = S^{eff}\hbar\omega^{eff} =$ 0.218 eV and $S^{eff} = 1.18$, and $\lambda_q \approx 2\lambda_{S_0 \rightarrow S_1} =$ 0.436 eV, see the Supporting Information for further details). The remaining normal modes can be treated classically and are included in λ_c, which is calculated as the difference between λ and λ_q (0.153 eV).

Table 1 gathers the exciton transfer rates computed at 300 K from eq 1 for the two non-equivalent molecular pairs shown in Figure 1. As expected, the fastest exciton transfer rate is obtained for the slipped π-stacked dimer of anthracene (dimer A) since it presents the strongest excitonic coupling. In this case, the thermal fluctuation does not have a significant impact on the exciton transfer rate causing a modest increase from 1.72×10^{12} s^{-1} to 1.86×10^{12} s^{-1} (Table 1). For dimer B instead, the hopping rate increases from 0.07×10^{12} s^{-1} to 0.75×10^{12} s^{-1} when the fluctuation of the excitonic coupling is included, because in this case the magnitude of the fluctuation is larger than the average coupling.

Table 1. Square of the excitonic couplings (eV^2) and exciton transfer rates (s^{-1}) computed for anthracene dimers. Exciton transfer rates without thermal fluctuation have been included for comparison.

Dimers	$\langle J^2 \rangle$	k	$\langle J \rangle^2$	k
A	1.33×10^{-3}	1.86×10^{12}	1.23×10^{-3}	1.72×10^{12}
B	5.33×10^{-4}	0.75×10^{12}	4.90×10^{-5}	0.07×10^{12}

The elements of the diffusion tensor (and the average diffusion coefficients) can be computed in the *ab* plane of anthracene from the hopping rates (see Figure S2 and the corresponding derivation in the Supporting Information). The average exciton diffusion coefficient for anthracene in the crystal *ab* plane, which is computed as the average of the diagonal elements of the tensor, is found to be $D = 5.6 \times 10^{-3}$ cm^2 s^{-1}. The exciton diffusion length (L_D) can be calculated by using the relationship $L_D = \sqrt{2D\tau}$,[67,68] where τ corresponds to the lifetime of the lowest Frenkel exciton. By assuming $\tau = 10$ ns,[69] an exciton diffusion length of 106 nm is obtained. Both exciton diffusion coefficients and exciton diffusion lengths are in good agreement with the experimental values ($D \sim 4.0$–6.0×10^{-3} cm^2 s^{-1} and $L_D \sim 90$–110 nm) estimated in the same *ab* plane from surface quenching and photocurrent measurements.[58,69]

It is also interesting to analyze the anisotropy of exciton transport. The exciton diffusion coefficient components along the *a* and *b* directions are computed as $D_a = 2.9 \times 10^{-3}$ and $D_b = 8.2 \times 10^{-3}$ cm^2 s^{-1} (Table 2). Assuming the same lifetime for the FE exciton ($\tau = 10$ ns), the exciton diffusion lengths in each direction, L_{D_a} and L_{D_b}, are calculated to be 76 and 128 nm, respectively. Experimental values for the exciton

diffusion lengths along the axis *a* and *b* were reported by Mulder *et al*. (60 and 100 nm, respectively).[70] It should be stressed that we have obtained a ratio between the exciton diffusion lengths along axis *a* and *b* (L_{D_a}/L_{D_b} ~ 0.6) similar to that experimentally observed only when the thermal fluctuations of the excitonic coupling were taken into account (L_{D_a}/L_{D_b} would be ~ 0.2 without the fluctuation effect, Table 2). This finding therefore highlights that the thermal fluctuation of the excitonic coupling is an important ingredient to predict quantitatively the exciton diffusion properties in organic molecular crystals.

Table 2. Exciton diffusion coefficients D ($cm^2\ s^{-1}$) and exciton diffusion lengths L_D (nm) computed for anthracene. Experimental estimates are also included.

Direction	Calculated		Experimental
	Fluctuation	No Fluctuation	
D			
ab	5.6×10^{-3}	3.3×10^{-3}	~ 4.0–6.0 × 10^{-3}[a]
a	2.9×10^{-3}	0.3×10^{-3}	1.8×10^{-3}[b]
b	8.2×10^{-3}	6.3×10^{-3}	5.1×10^{-3}[b]
L_D			
ab	106	81	~ 90–110[c]
a	76	23	60[b]
b	128	112	100[b]

[a] Values taken from ref. [69] and [58]. [b] Values from ref. [70]. [c] Estimated by using $L_D = \sqrt{2D\tau}$ with $\tau = 10$ ns.

3.4 Exciton transport in the coherent regime: the case of DCVSN5

When $J > \lambda/4$, as in DCVSN5, the local electron-phonon strength is not sufficient to form a small exciton-polaron, e.g. the lowest excited state of a dimer is delocalized,

with the molecular pair sharing the excitation.[71] In the absence of other effects, such as the fluctuation of *J*, the exciton remains delocalized in the solid and is well described by an excitonic band. If the fluctuations, i.e. the non-local electron-phonon couplings, are small, the description remains qualitatively similar and the effect of the non-local electron-phonon coupling is to renormalize the excitonic bands.[22] For the large fluctuations present in these materials, however, there is no simple analytical theory. Most of our understanding derives from theoretical and experimental work carried out in the past few years on the related problem of charge dynamics subject to the large fluctuation of hopping integrals, which is a formally identical problem if one can assume that there is only one important excited state per molecule. We know that the effect of the dynamic disorder is to localize the quasi-particle;[13] however, this is only a transient localization[72] and the dynamics of the quasi-particles is at the same time limited but also driven by the fluctuation.[73,74] Charge modulation spectroscopy[75] and Hall effect measurements[76] suggest that the charge carriers are at the same time localized and evolving coherently, supporting the idea that a transient localization takes place but the electronic coherence is preserved. In what follows we adapt the method originally developed to study charge transport in molecular crystals in the coherent limit to the problem of exciton transport in the same limit.

The transport in the DCVSN5 crystal can be assumed to take place mainly within columns (1D transport, Figure 4a) due to the strong excitonic coupling found for the antiparallel π-stacked pair with respect to the intercolumnar excitonic couplings for dimers B and C (Figure 3). In this context, a simplified model Hamiltonian able to incorporate the different physical ingredients for the exciton transport but with a reduced number of degrees of freedom can be derived. This model Hamiltonian is written as:

$$
\begin{aligned}
H = & \sum_{j}^{N}\left(E_j + \sum_k g^{(k)} q_j^{(k)} \right) |j\rangle\langle j| \\
& + \sum_{j}^{N}\left(J + \sum_k a^{(k)} (q_{j+1}^{(k)} - q_j^{(k)}) \right) \left(|j\rangle\langle j+1| + |j+1\rangle\langle j| \right) \\
& + \sum_{j}^{N}\sum_k \left(\frac{1}{2} m^{(k)} \left(\dot{q}_j^{(k)} \right)^2 + \frac{1}{2} m^{(k)} \left(\omega^{(k)} q_j^{(k)} \right)^2 \right)
\end{aligned}
\tag{2}
$$

The index j runs over the molecular sites in the 1D assemble (Figure 4a). On each molecule, only a single excited state $|j\rangle$ and several harmonic nuclear vibrations (indexed with k, with displacement $q_j^{(k)}$, effective mass $m^{(k)}$ and frequency $\omega^{(k)}$) are considered. At equilibrium position ($q_j^{(k)} = 0$), E_j and J denote the energy of the lowest singlet excited state and the excitonic couplings between these excited states at adjacent molecular sites. The nuclear vibrations in this model Hamiltonian are coupled to the exciton carriers in two different ways. The nuclear vibration $q_j^{(k)}$ modifies the exciton energy at site $|j\rangle$ according to the linear local exciton-phonon coupling (Holstein coupling[77]) term $g^{(k)} q_j^{(k)} |j\rangle\langle j|$, where $g^{(k)}$ is the local exciton-phonon constant and is related to the reorganization energy. On the other hand, the relative displacements between $q_j^{(k)}$ and $q_{j+1}^{(k)}$ modulate the excitonic coupling between the sites $|j\rangle$ and $|j+1\rangle$ with the term $a^{(k)}(q_{j+1}^{(k)} - q_j^{(k)})$ where $a^{(k)}$ quantifies the nonlocal electron-phonon coupling and can be related with the magnitude of the thermal fluctuation of the excitonic coupling.

Similar to the exciton transfer rate parameters for anthracene, the parameters in the model Hamiltonian are derived from first principle calculations and classical molecular dynamic simulations. For the diagonal parameters, E_j is set to 0 since each molecular site has the same energy value. The local Holstein electron-phonon constant g can be related to the reorganization energy and the corresponding Huang-Rhys factors. The

analysis of the Huang-Rhys factors computed at ωB97X-D/6-31G** for DCVSN5 (Figure S1) displays that only three normal modes at around 43, 600 and 1625 cm^{-1} couple strongly with the first electronic transition. These modes, mainly involving the stretching of the molecule along the long and short molecular axis and the stretching of the C-C/C=C bonds, are responsible for the vibronic progressions experimentally observed and computed for related oligothienoacenes.[78,79] Similar in spirit to other works,[13,80] a single effective vibration can be associated to the total reorganization energy of DCVSN5 (0.328 eV, 2645 cm^{-1}) and we set the frequency of the single effective mode to $\omega^{(1)} =$ 1400 cm^{-1} and the mass $m^{(1)} = 6$ amu (the reduced mass of the C-C/C=C bonds that gives the larger contribution to these modes). The local Holstein exciton-phonon constant is therefore computed by $g^{(1)} = \omega^{(1)}\sqrt{m^{(1)}\lambda} =$ 21484 cm^{-1} $Å^{-1}$ and the Huang-Rhys factor associated with this effective normal mode is computed to be 0.94.

For the off-diagonal term, *J* is set to be the average excitonic coupling ($\langle J \rangle = -0.200$ eV) computed in Section 3.1 for the antiparallel π-stacked dimer of DCVSN5. Table 3 collects all the parameters used for DCVSN5. Similar to the local exciton-phonon coupling, it is also convenient to select an effective mode that can capture the overall effect of the low-frequency vibrations on the excitonic coupling in the model Hamiltonian (eq 2). The Fourier transformation of the autocorrelation function $\langle \delta J(0)\delta J(t) \rangle$ (Figure 3) showed that the low-frequency vibrations (30–100 cm^{-1} range) modulate the excitonic coupling for DCVSN5, providing a broad distribution of the excitonic coupling. Therefore, we set $\omega^{(2)} = 50$ cm^{-1} as the vibrational frequency of the effective mode coupled strongly to the excitonic coupling. The mass of this effective vibration is set to be $m^{(2)} = 510$ amu, which corresponds to the mass of the DCVSN5

compound. An appropriate value for the nonlocal exciton-phonon coupling constant $a^{(2)}$ can be calculated if it is assumed that only the effective mode couples with *J*. In this case, the standard deviation of the excitonic coupling can be related to $a^{(2)}$ by $\sigma_J = a^{(2)}\sqrt{2k_BT/m^{(2)}(\omega^{(2)})^2}$. Using the standard deviation previously computed for the antiparallel π-stacked dimer of DCVSN5 (σ_J = 218 cm^{-1}), $a^{(2)}$ is found to be 2075 cm^{-1} Å^{-1}.

It is worth noting at this point that $(2\lambda_{S_0\rightarrow S_1}k_BT)^{1/2}$, where $\lambda_{S_0\rightarrow S_1}$ corresponds to the relaxation energy of the isolated DCVSN5 and related to the total reorganization energy (see the Supporting Information), can be interpreted as the amplitude of the fluctuation of the on-site exciton energies for the isolated DCVSN5 molecule according to Gerischer's formulation of Marcus theory.[81,82] Therefore, our model includes both diagonal (on-site energies) and off-diagonal (excitonic couplings) fluctuations of the electronic Hamiltonian on equal footing, the two terms being respectively the second and fourth term in eq 2.

Table 3. Parameters used for DCVSN5.

Parameter	Value	Description
N	800	Molecular sites
J	1613 cm^{-1}	Excitonic coupling
$g^{(1)}$	21484 cm^{-1} Å^{-1}	Holstein electron-phonon coupling (mode 1)
$\omega^{(1)}$	1400 cm^{-1}	Frequency of mode (1)
$m^{(1)}$	6 amu	Mass of mode (1)
$\alpha^{(2)}$	2075 cm^{-1} Å^{-1}	Peierls electron-phonon coupling (mode 2)
$\omega^{(2)}$	50 cm^{-1}	Frequency of mode (2)
$m^{(2)}$	510 amu	Mass of mode (2)

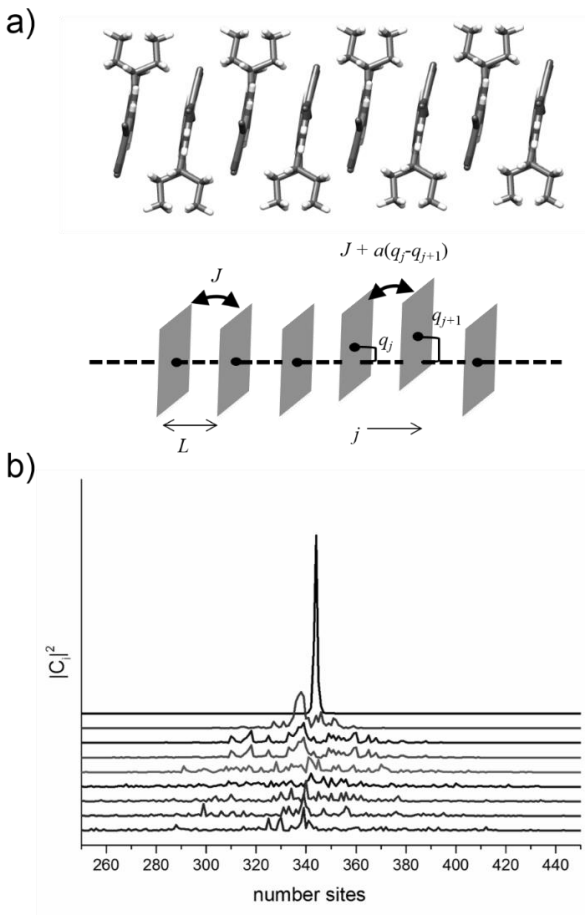

Figure 4. Scheme of the 1D model used to describe the exciton transport in the DCVSN5 crystal (a) and time evolution of the exciton wavefunction evaluated from the model Hamiltonian (b). Population on each site (vertically off-set for clarity) are reported from t=0 (top curve) to t=1 ps (bottom curve) every 0.125 ps.

The time evolution of the exciton wavefunction can be computed by integrating the model Hamiltonian (eq 2) within an Ehrenfest dynamics scheme, where the nuclear modes are treated classically as described in eq 2. Therefore, the equation of motion of the nuclear positions can be expressed by

$$m^{(k)}\ddot{q}_j^{(k)} = -m^{(k)}\left(\omega^{(k)}\right)^2 q_j^{(k)} - \frac{\partial}{\partial q_j^{(k)}}\left\langle \psi_n(t)\middle| H^{\mathrm{el}} \middle|\psi_n(t)\right\rangle \qquad (3)$$

H^{el} denotes the electronic Hamiltonian (the first two terms in eq 2) and $\psi_n(t)$ corresponds to the time-dependent exciton wavefunction. The last term in eq. 3

therefore represents the effect of the electronic Hamiltonian (H^{el}) coupled to the molecular vibrations on the nuclear degrees of freedom. Initial positions, $\left\{q_j^{(k)}(0)\right\}$, and velocities, $\left\{\dot{q}_j^{(k)}(0)\right\}$, of the nuclei are chosen from the Boltzmann distribution at room temperature. Further details of the numerical integration can be found for example in ref. [13]. The Ehrenfest procedure has some important limitations extensively discussed in literature,[74] most remarkably the absence of decoherence effects and erroneous equilibration at long times. On the other hand, it is preferable over surface hopping methods[83] when a quasi continuum of electronic states is present, as in this case.[84,85] It is generally acknowledged that further methodological improvements are necessary and we simply resort here to one of the best and straightforward options currently available.

Figure 4b displays the time evolution of the exciton wavefunction. The initial exciton wavefunction, which is selected to be in one of the excitonic eigenstates of the Hamiltonian at the beginning of the simulation, is localized just on a few sites (< 10) at 300 K. The initial localization of the exciton wavefunction is induced by disorder in the diagonal and off-diagonal terms of the electronic Hamiltonian. Nevertheless, the exciton wavefunction spreads quickly as a consequence of the time dependence of the excitonic couplings.

A quantitative study of the exciton diffusion along the columns of the DCVSN5 system can be performed by monitoring

$$R_n^2(t) \equiv \langle \psi_n(t) | r^2 | \psi_n(t) \rangle - \langle \psi_n(t) | r | \psi_n(t) \rangle^2 \qquad (4)$$

which measures the time-dependent spread of the wavefunction. $R_n^2(t)$ is computed from 77 different initial wavefunctions $\psi_n(0)$ (and energy E_n) and averaged (with Boltzmann weight) to give $\langle R^2(t) \rangle$. The diffusion constant is then evaluated from the relationship $D = \lim_{t\to\infty} \langle R^2(t) \rangle / 2t$ where the distance between molecules is set to 3.5

Å (average intermolecular distance between the DCVSN5 molecules within the antiparallel π-staked column Figure 2c). A value of D = 1.9 cm^2 s^{-1} is obtained for DCVSN5, which is almost three orders of magnitude larger than that computed for anthracene. This much more efficient exciton diffusion for DCVSN5 may explain why this compound and other related A-D-A oligothiophene derivatives exhibit remarkable efficiencies[37–40,86] when they are used in SM-OSCs. In many molecular materials, the exciton transport takes place via hopping and the slow exciton diffusion to the donor-acceptor interface in SM-OSC is one of the main efficiency loss mechanisms. In DCVSN5 one can speculate that the exciton can reach the donor-acceptor interface with extremely high quantum yields.

It can be worth stressing that the computation of exciton diffusion assuming incoherent transport in the case of DCVSN5 would yield completely unacceptable results. The exciton hopping rate would exceed 1.8 × 10^{14} s^{-1}, i.e. faster than any vibrational relaxation rate and therefore incompatible with any rate theory. The diffusion coefficient would also be about 10 times smaller, i.e. the differences between DCVSN5 and anthracene diffusivity cannot be derived simply by looking at the exciton coupling by looking at the relative exciton coupling strength.

4. Conclusions

In this contribution, we have explored the role of the thermal nuclear motion (dynamic disorder) on the exciton transport properties of organic molecular crystals in the limiting regimes of incoherent and coherent transport. Two different molecular crystals anthracene and a dicyanovinyl-capped *S*,*N*-heteropentacene derivative (DCVSN5) have been selected to be representative of the two regimes at room temperature.

Both anthracene and DCVSN5 exhibit a significant fluctuation of the excitonic couplings at room temperature owing to low-frequency intermolecular vibrations in the

20–100 cm^{-1} range. The impact of the modulation of the excitonic coupling on the transport properties is different in the incoherent and coherent regime. In anthracene, the exciton transport is shown to occur in the incoherent regime since the excitonic coupling between the lowest Frenkel excited states is much smaller than the reorganization energy for the exciton transfer process. A hopping rate expression that takes into account the fluctuation of the coupling has been used to compute diffusion coefficients, which in good agreement with the experimentally available data. The effect of the fluctuation of the coupling modifies quantitatively the results and can be important to improve the agreement between models and experiment but does not change the fundamental physics as it has been described in recent theoretical works on the same materials.[87]

On the other hand, DCVSN5 presents a strong excitonic coupling between the π-stacked antiparallel columns and the exciton transport can be assumed to occur in the coherent regime. In this regime, much analogous to what is being investigated for the problem of charge transport in molecular materials, the fluctuations of the excitonic coupling causes an initial localization of the exciton wavefunction in just a few molecules. This exciton wavefunction spreads quickly, assisted by the low-frequency modes that modulate the excitonic couplings. This is a completely different physical mechanism of transport, which has not been considered so far and may be essential to explain the much higher efficiency of a class of molecular donors used in small molecule organic solar cells. Considering that the reorganization energy is associated with the fluctuation of the on-site energy,[81] one can imagine that the incoherent regime is the limit with on-site energy fluctuation are strong and dominant over the off-diagonal coupling while the coherent regime is promoted by weaker on-site fluctuations which makes on-site and off-diagonal fluctuations of similar importance.

An overview of existing computational data suggests that it is probably more common for an "average" molecular crystal to transport its excitons in the incoherent regime. This is because excitonic couplings are often similar in magnitude to that of anthracene and the reorganization energy decreases slowly with increasing the size of the molecule. So, maybe surprisingly, the excitonic transport is typically more incoherent than charge transport in high mobility molecular semiconductors, because of the typically lower coupling between excitons. Molecules like DCVSN5 can be therefore considered exceptions with this respect, but of great technological significance. Since its large excitonic coupling is due to the large transition dipole moment from ground to first excited state, alternative materials with properties similar to that of DCVSN5 can be found among the compounds that share a similarly bright $S_0 \rightarrow S_1$ optical transition.

Supporting Information

Supporting Information is available from the Wiley Online Library or from the authors.

Acknowledgements

This work was supported by a Marie Curie Intra European Fellowship within the 7th European Community Framework Programme (FP7-PEOPLE-2012-IEF-329513) and the European Research Council (Grant No. 615834). We are grateful to the Prof. E. Ortí (University of Valencia) for providing the computational facilities to perform the numerical calculations shown in this paper.

[1] A. S. Davydov, *Theory of Molecular Excitons*; Plenum: New York, 1971.

[2] V. May, O. Kühn, *Charge and Energy Transfer Dynamics in Molecular Systems*; WILEY-VCH Verlag GmbH & Co. KGaA: Weinheim, Germany, 2011.

[3] R. D. Harcourt, G. D. Scholes, K. P. Ghiggino, *J. Chem. Phys.* **1994**, *101*, 10521.

[4] H. Yamagata, D. S. Maxwell, J. Fan, K. R. Kittilstved, A. L. Briseno, M. D. Barnes, F. C. Spano, *J. Phys. Chem. C* **2014**, *118*, 28842.

[5] N. J. Hestand, R. Tempelaar, J. Knoester, T. L. C. Jansen, F. C. Spano, *Phys. Rev. B* **2015**, *91*, 195315.

[6] J. Krausko, J. K. Malongwe, G. Bičanová, P. Klán, D. Nachtigallová, D. Heger, *J. Phys. Chem. A* **2015**, *119*, 8565.

[7] T. Förster, *Ann. Phys.* **1948**, *437*, 55.

[8] G. D. Scholes, *Annu. Rev. Phys. Chem.* **2003**, *54*, 57.

[9] C.-P. Hsu, Z.-Q. You, H.-C. Chen, *J. Phys. Chem. C* **2008**, *112*, 1204.

[10] A. S. Eggeman, S. Illig, A. Troisi, H. Sirringhaus, P. A. Midgley, *Nat Mater* **2013**, *12*, 1045.

[11] J. Aragó, A. Troisi, *Phys. Rev. Lett.* **2015**, *114*, 026402.

[12] A. Troisi, G. Orlandi, *J. Phys. Chem. A* **2006**, *110*, 4065.

[13] A. Troisi, G. Orlandi, *Phys. Rev. Lett.* **2006**, *96*, 086601.

[14] N. Renaud, F. C. Grozema, *J. Phys. Chem. Lett.* **2015**, *6*, 360.

[15] T. Stangl, P. Wilhelm, D. Schmitz, K. Remmerssen, S. Henzel, S.-S. Jester, S. Höger, J. Vogelsang, J. M. Lupton, *J. Phys. Chem. Lett.* **2015**, *6*, 1321.

[16] S. Jang, Y.-C. Cheng, D. R. Reichman, J. D. Eaves, *J. Chem. Phys.* **2008**, *129*, 101104.

[17] A. Kolli, A. Nazir, A. Olaya-Castro, *J. Chem. Phys.* **2011**, *135*, 154112.

[18] H.-T. Chang, Y.-C. Cheng, *J. Chem. Phys.* **2012**, *137*, 165103.

[19] H. Haken, P. Reineker, *Zeitschrift für Phys.* **1972**, *249*, 253.

[20] H. Haken, G. Strobl, *Zeitschrift für Phys.* **1973**, *262*, 135.

[21] S. M. Vlaming, V. A. Malyshev, A. Eisfeld, J. Knoester, *J. Chem. Phys.* **2013**, *138*, 214316.

[22] R. W. Munn, R. Silbey, *J. Chem. Phys.* **1985**, *83*, 1843.

[23] R. C. Powell, R. G. Kepler, *J. Lumin.* **1970**, *1-2*, 254.

[24] M. D. Cohen, E. Klein, Z. Ludmer, *Chem. Phys. Lett.* **1976**, *37*, 611.

[25] D. Donati, J. O. Williams, *Mol. Cryst. Liq. Cryst.* **1978**, *44*, 23.

[26] J. S. Meth, C. D. Marshall, M. D. Fayer, *Solid State Commun.* **1990**, *74*, 281.

[27] S. R. Yost, E. Hontz, S. Yeganeh, T. Van Voorhis, *J. Phys. Chem. C* **2012**, *116*, 17369.

[28] E. V. Emelianova, S. Athanasopoulos, R. J. Silbey, D. Beljonne, *Phys. Rev. Lett.* **2010**, *104*, 206405.

[29] L. Grisanti, Y. Olivier, L. Wang, S. Athanasopoulos, J. Cornil, D. Beljonne, *Phys. Rev. B* **2013**, *88*, 035450.

[30] V. Stehr, B. Engels, C. Deibel, R. F. Fink, *J. Chem. Phys.* **2014**, *140*, 024503.

[31] V. Stehr, R. F. Fink, B. Engels, J. Pflaum, C. Deibel, *J. Chem. Theory Comput.* **2014**, *10*, 1242.

[32] H. Yamagata, J. Norton, E. Hontz, Y. Olivier, D. Beljonne, J. L. Brédas, R. J. Silbey, F. C. Spano, *J. Chem. Phys.* **2011**, *134*, 204703.

[33] J. J. Burdett, C. J. Bardeen, *Acc. Chem. Res.* **2013**, *46*, 1312.

[34] M. W. B. Wilson, A. Rao, B. Ehrler, R. H. Friend, *Acc. Chem. Res.* **2013**, *46*, 1330.

[35] A. Mishra, D. Popovic, A. Vogt, H. Kast, T. Leitner, K. Walzer, M. Pfeiffer, E. Mena-Osteritz, P. Bäuerle, *Adv. Mater.* **2014**, *26*, 7217.

[36] A. Mishra, P. Bäuerle, *Angew. Chem. Int. Ed. Engl.* **2012**, *51*, 2020.

[37] R. Fitzner, E. Mena-Osteritz, A. Mishra, G. Schulz, E. Reinold, M. Weil, C. Körner, H. Ziehlke, C. Elschner, K. Leo, M. Riede, M. Pfeiffer, C. Uhrich, P. Bäuerle, *J. Am. Chem. Soc.* **2012**, *134*, 11064.

[38] S. Haid, A. Mishra, M. Weil, C. Uhrich, M. Pfeiffer, P. Bäuerle, *Adv. Funct. Mater.* **2012**, *22*, 4322.

[39] R. Fitzner, E. Mena-Osteritz, K. Walzer, M. Pfeiffer, P. Bäuerle, *Adv. Funct. Mater.* **2015**, *25*, 1845.

[40] B. Kan, M. Li, Q. Zhang, F. Liu, X. Wan, Y. Wang, W. Ni, G. Long, X. Yang, H. Feng, Y. Zuo, M. Zhang, F. Huang, Y. Cao, T. P. Russell, Y. Chen, *J. Am. Chem. Soc.* **2015**, *137*, 3886.

[41] http://www.heliatek.com/newscenter/presse/page/4/.

[42] N. L. Allinger, F. Li, L. Yan, J. C. Tai, *J. Comput. Chem.* **1990**, *11*, 868.

[43] H. Do, A. Troisi, *Phys. Chem. Chem. Phys.* **2015**, DOI:10.1039/C5CP04328J.

[44] C. M. Breneman, K. B. Wiberg, *J. Comput. Chem.* **1990**, *11*, 361.

[45] A. D. MacKerell, D. Bashford, M. Bellott, R. L. Dunbrack, J. D. Evanseck, M. J. Field, S. Fischer, J. Gao, H. Guo, S. Ha, D. Joseph-McCarthy, L. Kuchnir, K. Kuczera, F. T. Lau, C. Mattos, S. Michnick, T. Ngo, D. T. Nguyen, B. Prodhom, W. E. Reiher, B. Roux, M. Schlenkrich, J. C. Smith, R. Stote, J. Straub, M. Watanabe, J. Wiórkiewicz-Kuczera, D. Yin, M. Karplus, *J. Phys. Chem. B* **1998**, *102*, 3586.

[46] N. Foloppe, A. D. MacKerell, Jr., *J. Comput. Chem.* **2000**, *21*, 86.

[47] http://dasher.wustl.edu/tinker/.

[48] J. Aragó, A. Troisi, *J. Chem. Phys.* **2015**, *142*, 164107.

[49] E. Hennebicq, G. Pourtois, G. D. Scholes, L. M. Herz, D. M. Russell, C. Silva, S. Setayesh, A. C. Grimsdale, K. Müllen, J.-L. Brédas, D. Beljonne, *J. Am. Chem. Soc.* **2005**, *127*, 4744.

[50] K. A. Kistler, F. C. Spano, S. Matsika, *J. Phys. Chem. B* **2013**, *117*, 2032.

[51] J.-D. Chai, M. Head-Gordon, *Phys. Chem. Chem. Phys.* **2008**, *10*, 6615.

[52] J.-D. Chai, M. Head-Gordon, *J. Chem. Phys.* **2008**, *128*, 084106.

[53] J. S. Binkley, J. A. Pople, W. J. Hehre, *J. Am. Chem. Soc.* **1980**, *102*, 939.

[54] J. Aragó, J. Sancho-García, E. Ortí, D. Beljonne, *J. Chem. Theory Comput.* **2011**, *7*, 2068.

[55] M. J. Frisch, G. W. Trucks, H. B. Schlegel, G. E. Scuseria, M. A. Robb, J. R. Cheeseman, G. Scalmani, V. Barone, B. Mennucci, G. A. Petersson, H. Nakatsuji, M. Caricato, X. Li, H. P. Hratchian, A. F. Izmaylov, J. Bloino, G. Zheng, J. L. Sonnenberg, M. Hada, M. Ehara, K. Toyota, R. Fukuda, J. Hasegawa, M. Ishida, T. Nakajima, Y. Honda, O. Kitao, H. Nakai, T. Vreven, J. A. Montgomery, J. E. Peralta, F. Ogliaro, M. Bearpark, J. J. Heyd, E. Brothers, K. N. Kudin, V. N. Staroverov, R. Kobayashi, J. Normand, K. Raghavachari, A. Rendell, J. C. Burant, S. S. Iyengar, J. Tomasi, M. Cossi, N. Rega, J. M. Millam, M. Klene, J. E. Knox, J. B. Cross, V. Bakken, C. Adamo, J. Jaramillo, R. Gomperts, R. E. Stratmann, O. Yazyev, A. J. Austin, R. Cammi, C. Pomelli, J. W. Ochterski, R. L. Martin, K. Morokuma, V. G. Zakrzewski, G. A. Voth, P. Salvador, J. J. Dannenberg, S. Dapprich, A. D. Daniels, O. Farkas, J. B. Foresman, J. V Ortiz, J. Cioslowski, D. J. Fox, Gaussian 09, Revision D.01. *Gaussian, Inc., Wallingford CT* **2009**.

[56] J.-L. Brédas, D. Beljonne, V. Coropceanu, J. Cornil, *Chem. Rev.* **2004**, *104*, 4971.

[57] H. C. Wolf, In *Advances in Atomic and Molecular Physics*; Academic Press, New York, 1968; Vol. 3, pp. 119–142.

[58] A. Köhler, H. Bässler, *Electronic Processes in Organic Semiconductors: An Introduction*; WILEY-VCH Verlag GmbH & Co. KGaA: Weinheim, Germany, 2015.

[59] J. Tang, *J. Chem. Phys.* **1993**, *98*, 6263.

[60] I. A. Goychuk, E. G. Petrov, V. May, *J. Chem. Phys.* **1995**, *103*, 4937.

[61] E. S. Medvedev, A. A. Stuchebrukhov, *J. Chem. Phys.* **1997**, *107*, 3821.

[62] A. Troisi, A. Nitzan, M. A. Ratner, *J. Chem. Phys.* **2003**, *119*, 5782.

[63] Y. A. Berlin, F. C. Grozema, L. D. A. Siebbeles, M. A. Ratner, *J. Phys. Chem. C* **2008**, *112*, 10988.

[64] R. P. Fornari, J. Aragó, A. Troisi, *J. Chem. Phys.* **2015**, *142*, 184105.

[65] P. F. Barbara, T. J. Meyer, M. A. Ratner, *J. Phys. Chem.* **1996**, *100*, 13148.

[66] V. Coropceanu, J. Cornil, D. A. da Silva, Y. Olivier, R. Silbey, J. L. Brédas, *Chem. Rev.* **2007**, *107*, 926.

[67] O. V. Mikhnenko, H. Azimi, M. Scharber, M. Morana, P. W. M. Blom, M. A. Loi, *Energy Environ. Sci.* **2012**, *5*, 6960.

[68] Although the proper dimensionality factor in the exciton diffusion length expression for a 2D system would be 4 instead of 2, the factor of 2 was used in the experimental estimates. For consistence, we have employed the same dimensionality factor.

[69] R. C. Powell, Z. G. Soos, *J. Lumin.* **1975**, *11*, 1.

[70] B. J. Mulder, *Philips Res. Rept.* **1967**, *22*, 142.

[71] F. Fassioli, R. Dinshaw, P. C. Arpin, G. D. Scholes, *J. R. Soc. Interface* **2014**, *11*, 20130901.

[72] S. Ciuchi, S. Fratini, D. Mayou, *Phys. Rev. B* **2011**, *83*, 081202.

[73] S. Fratini, S. Ciuchi, D. Mayou, *Phys. Rev. B* **2014**, *89*, 235201.

[74] S. Fratini, D. Mayou, S. Ciuchi, *arXiv:1505.02686* **2015**.

[75] T. Sakanoue, H. Sirringhaus, *Nat. Mater.* **2010**, *9*, 736.

[76] J.-F. Chang, T. Sakanoue, Y. Olivier, T. Uemura, M.-B. Dufourg-Madec, S. G. Yeates, J. Cornil, J. Takeya, A. Troisi, H. Sirringhaus, *Phys. Rev. Lett.* **2011**, *107*, 066601.

[77] T. Holstein, *Ann. Phys. (N. Y).* **1959**, *8*, 325.

[78] J. Aragó, P. M. Viruela, E. Ortí, R. Malavé Osuna, B. Vercelli, G. Zotti, V. Hernández, J. T. López Navarrete, J. T. Henssler, A. J. Matzger, Y. Suzuki, S. Yamaguchi, *Chem. – A Eur. J.* **2010**, *16*, 5481.

[79] J. Aragó, P. M. Viruela, J. Gierschner, E. Ortí, B. Milián-Medina, *Phys. Chem. Chem. Phys.* **2011**, *13*, 1457.

[80] J. Jortner, *J. Chem. Phys.* **1976**, *64*, 4860.

[81] H. Gerischer, *Z. Phys. Chem.* **1960**, *26*, 223.

[82] R. P. Fornari, A. Troisi, *Phys. Chem. Chem. Phys.* **2014**, *16*, 9997.

[83] J. C. Tully, *J. Chem. Phys.* **1990**, *93*, 1061.

[84] L. Wang, A. V Akimov, L. Chen, O. V Prezhdo, *J. Chem. Phys.* **2013**, *139*, 174109.

[85] A. V. Akimov, R. Long, O. V. Prezhdo, *J. Chem. Phys.* **2014**, *140*, 194107.

[86] R. Fitzner, C. Elschner, M. Weil, C. Uhrich, C. Körner, M. Riede, K. Leo, M. Pfeiffer, E. Reinold, E. Mena-Osteritz, P. Bäuerle, *Adv. Mater.* **2012**, *24*, 675.

[87] G. M. Akselrod, P. B. Deotare, N. J. Thompson, J. Lee, W. A. Tisdale, M. A. Baldo, V. M. Menon, V. Bulović, *Nat Commun* **2014**, *5*, 3646.

Table of Contents Graphics

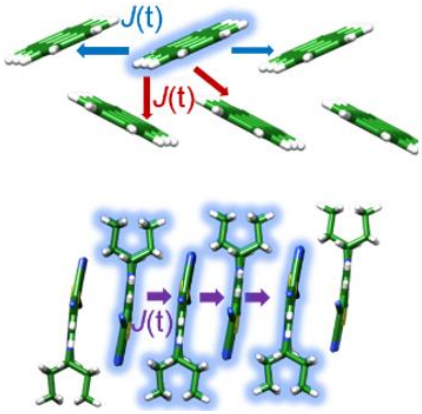

Thermal motions in molecular crystals cause substantial fluctuation of the excitonic coupling between neighboring molecules (dynamic disorder) and, thus, the role of this fluctuation on the exciton dynamics is explored in two extreme regimes (incoherent and coherent) by means of two crystal models, anthracene and a heteropentacene derivative.